in Proc. IEEE SPAWC-09
Perugia, Italy, June 2009, pp. 1-5

SEQUENTIAL LSQR-BASED ICI EQUALIZATION AND DECISION-FEEDBACK ISI CANCELLATION IN PULSE-SHAPED MULTICARRIER SYSTEMS

Mario Hampejs,[a] Pavol Švač,[b] Georg Tauböck,[b] Karlheinz Gröchenig,[a] Franz Hlawatsch,[b] and Gerald Matz[b]

[a]Numerical Harmonic Analysis Group, University of Vienna
Nordbergstrasse 15, A-1090 Vienna, Austria; e-mail: karlheinz.groechenig@univie.ac.at

[b]Institute of Communications and Radio-Frequency Engineering, Vienna University of Technology
Gusshausstrasse 25/389, A-1040 Vienna, Austria; e-mail: pavol.svac@nt.tuwien.ac.at

ABSTRACT

We propose a frequency-domain method for equalizing intercarrier interference (ICI) and intersymbol interference (ISI) in multicarrier transmissions over rapidly time-varying and strongly delay-spread channels. Postcursor ISI is cancelled by a decision-feedback structure, and ICI is equalized by a sequential version of the recently proposed LSQR equalizer, based on a band approximation for the frequency-domain channel matrix. The sequential LSQR equalizer uses an interference cancellation scheme with reliability-based sorting of sets of subcarriers. This approach is shown to yield excellent performance at moderate complexity. A pulse-shaped multicarrier system is considered because of its generality and advantages. This framework includes cyclic-prefix OFDM as a special case.

1. INTRODUCTION

Orthogonal frequency division multiplexing (OFDM) systems have recently been studied in the context of rapidly time-varying channels, an example being mobile reception of DVB-T [1]. In highly mobile scenarios, large Doppler shifts cause nonnegligible intercarrier interference (ICI). As demonstrated e.g. in [2–4], using *pulse-shaped* multicarrier (PS-MC) modulation [2, 3, 5–8] with smooth transmit and receive pulses can lead to a substantial reduction of ICI compared to conventional cyclic-prefix (CP) OFDM.

Most ICI equalization methods operate in the frequency domain and process all subcarriers [9] or a few neighboring subcarriers [10, 11] simultaneously. The latter methods achieve low complexity by exploiting the (approximate) band structure of the frequency-domain channel matrix. The band approximation is more accurate for well-designed PS-MC systems than for CP-OFDM systems [4].

Two recently proposed ICI equalization methods [4, 12] use the iterative *LSQR algorithm* [13] and exploit the band structure of, respectively, the frequency-domain and time-domain channel matrix to reduce complexity. The LSQR algorithm is a conjugate-gradient method that exhibits excellent performance due to its inherent regularization capability. The frequency-domain LSQR equalizer [4] is more efficient than its time-domain counterpart [12] for channels with potentially large delays as, e.g., in single-frequency DVB-T networks. However, large channel delays tend to produce *intersymbol interference* (ISI) in addition to ICI, especially in PS-MC systems that use well frequency-concentrated (thus, long) pulses to keep ICI low. In this case, the ISI has to be equalized along with the ICI.

This work was supported by WWTF project MA 44 (MOHAWI) and by STREP project MASCOT (IST-026905) within the Sixth Framework Programme of the European Commission.

In this paper, we propose a frequency-domain ICI/ISI equalizer for doubly selective channels that are both rapidly time-varying and highly delay-spread. Our equalizer embeds an improved frequency-domain LSQR-based ICI equalizer in a decision-feedback equalizer (DFE) structure that cancels postcursor ISI. DFEs for ISI cancellation have been previously proposed together with other ICI equalization methods [14, 15]. They are attractive due to their moderate complexity and reduced noise enhancement. We do not use soft ISI cancellation because, as will be shown in Section 4, the performance of the proposed method is already excellent.

For ICI equalization, we propose a new "sequential" version of the LSQR algorithm (termed the *S-LSQR algorithm*), which exhibits excellent performance at moderate complexity. The S-LSQR algorithm employs a multi-recursion extension of *selective parallel interference cancellation* (SPIC) [16] that uses a dynamic reliability criterion. At each recursion, a subset of subcarriers is detected and cancelled in an order defined by the reliability of the equalized symbols involved. This strategy was previously used in [17], however with a different reliability criterion. Existing works in a somewhat similar direction include [18], where postcursor ISI is also removed by a DFE but ICI is reduced by a conventional parallel interference cancellation scheme, and [19], which combines a sort of reliability-based ranking with a tree-search algorithm.

This paper is organized as follows. In Section 2, the system model is presented. In Section 3, we describe the architecture of the proposed ICI/ISI equalizer, discuss the new S-LSQR method, and address pulse design issues. Finally, simulation results are provided in Section 4. We consider a PS-MC system because of its generality and advantages. CP-OFDM is a special case of this framework.

2. SYSTEM MODEL

We assume a PS-MC system [2, 3] with K subcarriers and symbol period $N \geq K$ transmitting over a doubly selective channel. The equivalent discrete-time baseband system is considered throughout.

2.1. Modulator, channel, demodulator

The transmit signal produced by the modulator is of the form

$$s(n) = \sum_{l=-\infty}^{\infty} \sum_{k=0}^{K-1} a_{l,k}\, g_{l,k}(n)\,, \tag{1}$$

where $a_{l,k} \in \mathcal{A}$ ($l \in \mathbb{Z}$, $k \in \{0, \ldots, K-1\}$) denotes the complex data symbols, drawn from a finite symbol alphabet $\mathcal{A}$, and

$$g_{l,k}(n) \triangleq g(n-lN)\, e^{j2\pi \frac{k}{K}(n-lN)}$$

is a time-frequency shifted version of a transmit pulse $g(n)$. Assuming a doubly selective channel with maximum delay M, the received signal is

$$r(n) \;=\; (\mathbb{H}s)(n) + z(n) \;=\; \sum_{m=0}^{M} h(n,m)\, s(n-m) + z(n)\,, \tag{2}$$

where $h(n,m)$ denotes the time-varying impulse response of the channel $\mathbb{H}$ and $z(n)$ is white noise with variance σ_z^2. Finally, the demodulator computes the inner products

$$x_{l,k} \;=\; \langle r, \gamma_{l,k} \rangle \;=\; \sum_{n=-\infty}^{\infty} r(n)\, \gamma_{l,k}^*(n)\,, \tag{3}$$

where $\gamma_{l,k}(n) \triangleq \gamma(n-lN)\, e^{j2\pi \frac{k}{K}(n-lN)}$ is a time-frequency shifted version of a receive pulse $\gamma(n)$. If $g(n)$ is a rectangular pulse on the interval $[0, N-1]$ and $\gamma(n)$ is a rectangular pulse on the interval $[N-K, N-1]$, the PS-MC system reduces to a conventional CP-OFDM system with CP length $N-K$.

2.2. Equivalent channel

Combining (1), (2), and (3), we obtain the following symbol-level input-output relation [2]:

$$x_{l,k} \;=\; \sum_{l'=-\infty}^{\infty} \sum_{k'=0}^{K-1} H_{l,k;l',k'}\, a_{l',k'} \;+\; z_{l,k}\,, \tag{4}$$

where $H_{l,k;l',k'}$ can be expressed in terms of $h(n,m)$, $g(n)$, and $\gamma(n)$ [2] and $z_{l,k} = \langle z, \gamma_{l,k} \rangle$. Relation (4) describes the *equivalent channel* that includes the modulator, physical channel, and demodulator. In particular, $H_{l,k;l',k'}$ expresses ICI for $k \neq k'$ and $l = l'$ and ISI for $l \neq l'$. The system channel (4) can be compactly written as

$$\mathbf{x}_l \;=\; \sum_{\lambda=-\infty}^{\infty} \mathbf{H}_{l,\lambda}\, \mathbf{a}_{l-\lambda} \;+\; \mathbf{z}_l\,, \qquad l \in \mathbb{Z}\,,$$

with $\mathbf{x}_l \triangleq [x_{l,0} \cdots x_{l,K-1}]^T$, $\mathbf{a}_l \triangleq [a_{l,0} \cdots a_{l,K-1}]^T$, and $\mathbf{z}_l \triangleq [z_{l,0} \cdots z_{l,K-1}]^T$ and the *frequency-domain channel matrices* $\mathbf{H}_{l,\lambda}$ of size $K \times K$ whose entries are $(\mathbf{H}_{l,\lambda})_{k,k'} = H_{l,k;l-\lambda,k'}$. The ICI is described by the off-diagonal entries of the matrices $\mathbf{H}_{l,0}$, which are small if they are not too close to the main diagonal and if the pulses $g(n)$ and $\gamma(n)$ are suitably designed. This suggests to approximate $\mathbf{H}_{l,0}$ by a *(quasi-)banded matrix* $\widetilde{\mathbf{H}}_{l,0}$ defined by

$$(\widetilde{\mathbf{H}}_{l,0})_{k,k'} \triangleq \begin{cases} (\mathbf{H}_{l,0})_{k,k'}\,, & |k'-k| \leq B \;\text{ or }\; |k'-k| \geq K-B\,, \\ 0\,, & \text{otherwise}\,, \end{cases} \tag{5}$$

i.e., a matrix with a band of one-sided width B about the main diagonal and two bands of width B in the lower-left and upper-right corners [4, 7, 8].

The ISI is described by all nonzero channel matrices $\mathbf{H}_{l,\lambda}$ for $\lambda \neq 0$; it consists of *postcursor* ISI ($\lambda > 0$) and *precursor* ISI ($\lambda < 0$). For the special case of CP-OFDM, ISI is avoided if the CP length $N-K$ is not smaller than the maximum channel delay M. For general PS-MC systems, some ISI will usually be present; the amount of ISI depends on the channel and the transmit and receive pulses. Hereafter, we assume finite-length, causal pulses $g(n)$ and $\gamma(n)$ with supports $[0, L_g-1]$ and $[0, L_\gamma-1]$, respectively. Then, the matrices $\mathbf{H}_{l,\lambda}$ can only be nonzero for $-L_{\text{pre}} \leq \lambda \leq L_{\text{post}}$, with $L_{\text{pre}} = \lfloor \frac{L_\gamma - 1}{N} \rfloor$ and $L_{\text{post}} = \lfloor \frac{L_g + M - 1}{N} \rfloor$. In practice, L_{pre} and L_{post} are usually between 0 and 2.

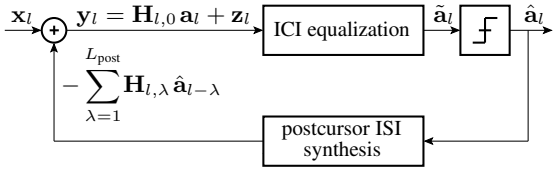

Fig. 1. DFE architecture for ICI/ISI equalization.

3. ICI/ISI EQUALIZER

As mentioned in Section 1, the proposed ICI/ISI equalizer operates in the frequency domain and uses a DFE architecture for postcursor ISI cancellation and a sequential extension of the LSQR algorithm for ICI equalization. The channel is assumed known.

3.1. ISI equalization

A DFE architecture [14, 15], depicted in Fig. 1, is adopted because of its computational efficiency and reduced noise enhancement. We assume $\hat{\mathbf{a}}_l = \mathbf{a}_l$ (correct detection) and that precursor ISI is negligible (cf. Section 3.3). In the feedback branch of the DFE, a replica of postcursor ISI is generated from the L_{post} previously detected symbols and subtracted from the received signal. This yields

$$\mathbf{y}_l \;=\; \mathbf{x}_l - \sum_{\lambda=1}^{L_{\text{post}}} \mathbf{H}_{l,\lambda}\, \hat{\mathbf{a}}_{l-\lambda} \;=\; \mathbf{H}_{l,0}\, \mathbf{a}_l \;+\; \mathbf{z}_l\,, \tag{6}$$

where $\hat{\mathbf{a}}_l \in \mathcal{A}^K$ denotes the detected (quantized) symbol at time l. The last expression in (6) contains, besides the noise $\mathbf{z}_l$, only ICI as characterized by the matrix $\mathbf{H}_{l,0}$.

3.2. ICI equalization: The S-LSQR algorithm

In the feedforward branch of the DFE in Fig. 1, a linear equalizer combats the ICI present in $\mathbf{y}_l$ according to (6). For ICI equalization, we propose a novel sequential version of the LSQR algorithm. We model $\mathbf{H}_{l,0}$ by a quasi-banded matrix $\widetilde{\mathbf{H}}_{l,0}$ as defined in (5), so that the result of ISI cancellation in (6) is written as

$$\mathbf{y}_l \;=\; \widetilde{\mathbf{H}}_{l,0}\, \mathbf{a}_l \;+\; \mathbf{z}_l\,.$$

In what follows, we consider a fixed symbol time l and thus suppress the corresponding subscript for simplicity of notation.

Review of the LSQR algorithm. The basic LSQR equalizer can be motivated by the zero-forcing (ZF) equalizer, which produces the symbol vector estimate $\tilde{\mathbf{a}}_{\text{ZF}} = \widetilde{\mathbf{H}}^{-1}\mathbf{y}$. This estimate can also be formulated as the solution of a least-squares problem:

$$\tilde{\mathbf{a}}_{\text{ZF}} \;\triangleq\; \arg\min_{\mathbf{a} \in \mathbb{C}^K} \|\mathbf{y} - \widetilde{\mathbf{H}}\mathbf{a}\|^2.$$

The LSQR algorithm is an iterative method for solving large, sparse, possibly ill-conditioned least-squares problems [13]. At the ith iteration, it minimizes $\|\mathbf{y} - \widetilde{\mathbf{H}}\mathbf{a}\|^2$ subject to the constraint that $\mathbf{a}$ lies in the Krylov subspace spanned by the $i{+}1$ vectors $\widetilde{\mathbf{H}}^H\mathbf{y}$, $\widetilde{\mathbf{H}}^H\widetilde{\mathbf{H}}\widetilde{\mathbf{H}}^H\mathbf{y}$, …, $(\widetilde{\mathbf{H}}^H\widetilde{\mathbf{H}})^i\widetilde{\mathbf{H}}^H\mathbf{y}$ [20, Section 9.1.1]. A concise statement of the LSQR algorithm can be found e.g. in [4].

The LSQR algorithm exhibits good numerical stability, inherent regularization, and low computational complexity for sparse matrices. The matrix $\widetilde{\mathbf{H}}$ is sparse because it is quasi-banded, and it is notoriously ill-conditioned, especially for channels with large delay spread or Doppler spread. The ill-conditioning of $\widetilde{\mathbf{H}}$ calls for a regu-

larization, which can be achieved very easily by an early termination of the LSQR iterations [21]. This is because the initial iterations reduce the approximation error $\|\mathbf{y}-\widetilde{\mathbf{H}}\mathbf{a}\|$ in the directions of the dominant right singular vectors of $\widetilde{\mathbf{H}}$, which are least affected by noise. Due to the regularization, the performance of the LSQR equalizer with early termination is much better than that of the ZF equalizer (see [12] for a comparison with the MMSE equalizer). The complexity order is $\mathcal{O}(KBI)$, i.e., linear in the number of subcarriers K, matrix bandwidth B, and number of iterations I.

The S-LSQR algorithm. The proposed *S-LSQR equalizer* combines the LSQR equalizer with a multi-recursion extension of the SPIC scheme. SPIC [16] is a form of parallel interference cancellation that divides the equalized symbols into a reliable set and an unreliable set based on a comparison with a threshold. The reliable symbols are detected and cancelled, and all the unreliable symbols are detected in a second step from the interference-reduced received signal. The extended SPIC scheme employed by the S-LSQR equalizer uses several recursions to detect and cancel all subcarriers; at each recursion, the symbols are divided into a reliable set and an unreliable set based on a dynamic threshold comparison. Except for the reliability criterion, this is similar to *modified successive interference cancellation* [17], which cancels at each recursion the contribution of a subset of subcarriers with the highest SNR values.

The operation of the S-LSQR equalizer can be summarized as follows. At the first recursion, the LSQR equalizer is applied to $\mathbf{y}$. After quantization, we obtain the detected symbol vector $\hat{\mathbf{a}}^{(1)} \in \mathcal{A}^K$. Let $\hat{\boldsymbol{\alpha}}^{(1)} \in \mathcal{A}^{J_1}$ contain all detected symbols that satisfy a specific reliability criterion (to be defined below). The contribution of these symbols to $\mathbf{y}$ is subtracted from $\mathbf{y}$, i.e.,

$$\mathbf{y}^{(1)} = \mathbf{y} - \mathbf{G}^{(1)}\hat{\boldsymbol{\alpha}}^{(1)},$$

where the $K \times J_1$ matrix $\mathbf{G}^{(1)}$ is formed by the J_1 columns of $\widetilde{\mathbf{H}}$ corresponding to the symbols in $\hat{\boldsymbol{\alpha}}^{(1)}$. Assuming $\hat{\boldsymbol{\alpha}}^{(1)}$ to be correct, $\mathbf{y}^{(1)}$ is the received vector for a reduced system model

$$\mathbf{y}^{(1)} = \widetilde{\mathbf{H}}^{(1)}\mathbf{a}^{(2)} + \mathbf{z}\,. \tag{7}$$

Here, $\mathbf{a}^{(2)} \in \mathcal{A}^{K-J_1}$ is the subvector of $\mathbf{a}$ that contains all transmit symbols except those corresponding to $\hat{\boldsymbol{\alpha}}^{(1)}$, and $\widetilde{\mathbf{H}}^{(1)}$ contains the columns of $\widetilde{\mathbf{H}}$ corresponding to the symbols in $\mathbf{a}^{(2)}$ (in other words, $\widetilde{\mathbf{H}}^{(1)}$ is $\widetilde{\mathbf{H}}$ without the columns of $\mathbf{G}^{(1)}$).

At the second recursion, we tackle the reduced system (7) by applying the LSQR equalizer to $\mathbf{y}^{(1)}$, using $\widetilde{\mathbf{H}}^{(1)}$ as the system matrix. Quantization then yields $\hat{\mathbf{a}}^{(2)} \in \mathcal{A}^{K-J_1}$. Let $\hat{\boldsymbol{\alpha}}^{(2)} \in \mathcal{A}^{J_2}$ contain all detected symbols that satisfy our reliability criterion. The contribution of these symbols is subtracted from $\mathbf{y}^{(1)}$:

$$\mathbf{y}^{(2)} = \mathbf{y}^{(1)} - \mathbf{G}^{(2)}\hat{\boldsymbol{\alpha}}^{(2)},$$

where $\mathbf{G}^{(2)}$ is formed by the J_2 columns of $\widetilde{\mathbf{H}}$ corresponding to the symbols in $\hat{\boldsymbol{\alpha}}^{(2)}$. Assuming $\hat{\boldsymbol{\alpha}}^{(2)}$ to be correct, we have the reduced system model

$$\mathbf{y}^{(2)} = \widetilde{\mathbf{H}}^{(2)}\mathbf{a}^{(3)} + \mathbf{z}\,,$$

where $\mathbf{a}^{(3)} \in \mathcal{A}^{K-J_1-J_2}$ contains all transmit symbols except those corresponding to $\hat{\boldsymbol{\alpha}}^{(1)}$ and $\hat{\boldsymbol{\alpha}}^{(2)}$, and $\widetilde{\mathbf{H}}^{(2)}$ is formed by the columns of $\widetilde{\mathbf{H}}$ corresponding to the symbols in $\mathbf{a}^{(3)}$ (i.e., $\widetilde{\mathbf{H}}$ without the columns of $\mathbf{G}^{(1)}$ and $\mathbf{G}^{(2)}$).

The sequential algorithm proceeds in this fashion. At each recursion, it applies LSQR equalization and quantization to the current reduced system model and subtracts the contribution of the detected symbols satisfying the current reliability criterion from the current reduced version of $\mathbf{y}$. Error propagation is minimized by subtracting the contribution of the *most reliably* detected symbols at each recursion. This improves on previously proposed iterative ICI equalization schemes without reliability-based sorting [22, 23].

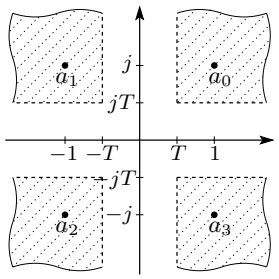

Fig. 2. Reliable zones for a QPSK constellation.

Reliability criterion. It remains to describe the reliability criterion used by the S-LSQR equalizer to select a set of most reliably detected symbols. Inspired by [16, 24], we define, in the complex symbol plane, a *reliable zone* (RZ) for each symbol of the signal constellation. The size of the RZs is defined by a single threshold parameter T. This is illustrated in Fig. 2 for a QPSK constellation (generalization to other QAM and PSK constellations is quite straightforward). At each recursion of the S-LSQR equalizer, a detected symbol is classified as *reliable* if the corresponding equalized symbol (i.e., before quantization) is located in one of the RZs. Note that the resulting decision metric can be considered as being intermediate between soft and hard due to the presence of dead zones separating the RZs. To reduce the number of recursions required (and, thus, the processing delay), we enlarge the RZs after each recursion by reducing T by a predefined value ε. Thus, the reliability criterion is changed dynamically between the recursions.

Complexity. The computational complexity of the S-LSQR equalizer is roughly of order $\mathcal{O}(KBIR)$, where I is the number of basic LSQR iterations and R is the number of recursions performed by the S-LSQR scheme. Here, R depends on the numbers J_r of symbols (subcarriers) processed at the individual recursions. The latter depend on the RZs at the individual recursions, which are defined by the sequence of threshold parameters T_r. If $T_1 = 0$, the RZs fill the entire complex plane (see Fig. 2), and thus $R = 1$ (all symbols are processed in a single recursion); the S-LSQR equalizer here reduces to the LSQR equalizer with complexity $\mathcal{O}(KBI)$. At the other extreme, it is possible theoretically that only a single symbol is processed at each recursion, and thus $R = K$. The complexity will then be $\mathcal{O}(K^2BI)$. Processing fewer symbols per recursion and, thus, using more recursions results in higher complexity but also in better performance up to a certain point. In fact, it is shown in Section 4 that increasing R beyond a relatively small value ($\ll K$) does not further improve the performance of the S-LSQR equalizer.

3.3. Pulse Design

The pulses $g(n)$ and $\gamma(n)$ should be designed such that precursor ISI and out-of-band ICI are minimized. We assume that the channel satisfies the wide-sense stationary uncorrelated scattering (WSSUS) property [25]. Following [3, 8], we minimize the reciprocal of the signal-to-interference-and-noise ratio (SINR) without a (bi)orthogonality constraint. The SINR is defined as $J(g,\gamma) \triangleq (\sigma_I^2 + \sigma_W^2)/\sigma_D^2$, with signal power $\sigma_D^2 \triangleq \mathrm{E}\{|H_{l,k;l,k}|^2\}$ and noise

power $\sigma_W^2 \triangleq \sigma_z^2 \sum_{n=0}^{L_\gamma-1} |\gamma(n)|^2$. Differently from [3, 8], we define the interference power σ_I^2 as

$$\sigma_I^2 \triangleq \sum_{\lambda=1}^{L_{\text{pre}}} \sum_{p=0}^{K-1} \mathrm{E}\left\{ |H_{l,k;l+\lambda,(k+p) \bmod K}|^2 \right\} + \sum_{|p|>B} \mathrm{E}\left\{ |H_{l,k;l,(k+p) \bmod K}|^2 \right\}.$$

(This does not depend on l, k because of the WSSUS assumption.) As in [26], σ_I^2 does not penalize in-band ICI and postcursor ISI. If postcursor ISI was penalized (by including $[-L_{\text{post}}, -1]$ in the λ summation interval), then, especially for large channel delays, very short pulses would be obtained. This would yield a high condition number of $\widetilde{\mathbf{H}}$ and, thus, poor ICI equalization performance.

The signal power can be calculated as [2–4]

$$\sigma_D^2 = \sum_{m=0}^{M} \int_{-\xi_{\max}/2}^{\xi_{\max}/2} C_{\mathbb{H}}(m,\xi)\, |A_{\gamma,g}(m,\xi)|^2\, d\xi,$$

where $C_{\mathbb{H}}(m,\xi)$ is the channel's scattering function [25] (which is assumed to be supported in the rectangle $[0, M] \times [-\xi_{\max}/2, \xi_{\max}/2]$) and $A_{\gamma,g}(m,\xi) \triangleq \sum_{n=-\infty}^{\infty} \gamma(n)\, g^*(n-m)\, e^{-j2\pi\xi n}$ is the cross-ambiguity function of the pulses. Similarly, the interference power can be calculated as

$$\sigma_I^2 = \sum_{m=0}^{M} \int_{-\xi_{\max}/2}^{\xi_{\max}/2} C_{\mathbb{H}}(m,\xi)\, P_{\gamma,g}^{(B)}(m,\xi)\, d\xi,$$

with

$$P_{\gamma,g}^{(B)}(m,\xi) \triangleq \sum_{\lambda=1}^{L_{\text{pre}}} \sum_{p=0}^{K-1} \left| A_{\gamma,g}\left(m+\lambda N, \xi+\frac{p}{K}\right) \right|^2 + \sum_{|p|>B} \left| A_{\gamma,g}\left(m, \xi+\frac{p}{K}\right) \right|^2.$$

Finally, $J(g,\gamma) = (\sigma_I^2 + \sigma_W^2)/\sigma_D^2$ is minimized by means of a numerical optimization routine.

4. SIMULATION RESULTS

Simulation setup. We simulated a PS-MC system with $K = 128$ subcarriers and symbol period $N = 144$, using a rate-1/2 convolutional code (generator polynomial $(13_8, 15_8)$), a 16×16 row-column interleaver, and a QPSK symbol alphabet with Gray labeling. A noisy WSSUS channel with brick-shaped scattering function (uniform delay and Doppler profiles) was simulated according to [27]. The channel's maximum delay M ranged between 10 and 56 (M/N between 6.9% to 38.9%), the maximum Doppler was $\xi_{\max} = 2{\cdot}10^{-3}$ (12.8% of the subcarrier spacing). This corresponds to a delay-Doppler spread $M\xi_{\max}$ between $2 \cdot 10^{-2}$ and $1.12 \cdot 10^{-1}$.

The transmit and receive pulses were designed individually for the various values of M as discussed in Section 3.3. The channel matrix bandwidth was chosen as $B = 10$. We set $\sigma_W^2 = 0$ for simplicity and used the resulting pulses for all SNR values. The iterative pulse optimization routine (function `fminunc` in Matlab's optimization toolbox) was initialized by a smooth orthogonal pulse of length 161 that was constructed according to [4]. The DFE length resulted as $L_{\text{post}} = 1$ for all M.

The S-LSQR algorithm performed $I = 16$ LSQR iterations. The threshold parameter T was initially set to $T_1 = 1.4$ and decreased by a fixed ε at the end of each recursion. Except for our last simulation experiment, we used $\varepsilon = 0.2$, resulting in at most $R = 8$ S-LSQR recursions. To keep complexity and latency low, the equalizer did not use channel decoding-reencoding in its feedback loops.

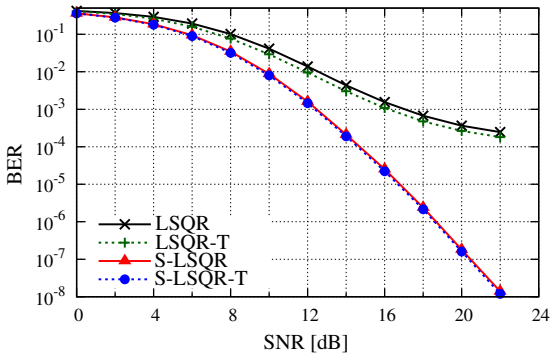

Fig. 3. BER of various ICI/ISI equalizers versus SNR, at $M/N = 34.7\%$.

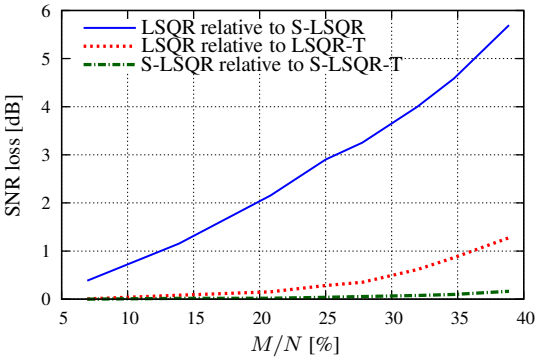

Fig. 4. SNR loss of various ICI/ISI equalizers relative to a reference method versus M/N, for a target BER of 10^{-3}.

BER versus SNR. Fig. 3 shows the bit-error rate (BER) of various ICI/ISI equalizers versus the SNR, at $M/N = 34.7\%$. We compare the DFEs with LSQR-based and S-LSQR-based ICI equalizer (abbreviated LSQR and S-LSQR) and their genie-aided counterparts with feedback of the true symbols (abbreviated LSQR-T and S-LSQR-T). It is seen that S-LSQR significantly outperforms LSQR. The performance gain is substantial at all SNRs but grows with the SNR. This shows that the generalized SPIC used by S-LSQR is very effective in combating the various impairments (ICI, residual ISI, band approximation error). It is furthermore seen that the BER loss of LSQR relative to LSQR-T (due to DFE error propagation) is small, and the BER loss of S-LSQR relative to S-LSQR-T is negligible. This shows that the DFE using the proposed S-LSQR algorithm does not suffer from error propagation.

SNR loss versus maximum channel delay. Fig. 4 shows the SNR loss of various methods relative to a reference method for a target BER of 10^{-3}, as a function of the maximum channel delay M. It is seen that LSQR requires a considerably higher SNR than S-LSQR to achieve the target BER. This SNR loss increases with M; e.g., it is about 3 dB at M/N =25% and about 5.7 dB at $M/N = 39\%$. Around $M/N = 39\%$, moreover, the BER of LSQR (as a function of the SNR) saturated in the vicinity of our target BER. Thus, for M/N larger than about 39%, LSQR (in contrast to S-LSQR) cannot achieve a BER of 10^{-3} even for very large SNR values.

The two lower curves of Fig. 4 quantify error propagation effects by displaying the SNR loss of LSQR and S-LSQR relative to LSQR-

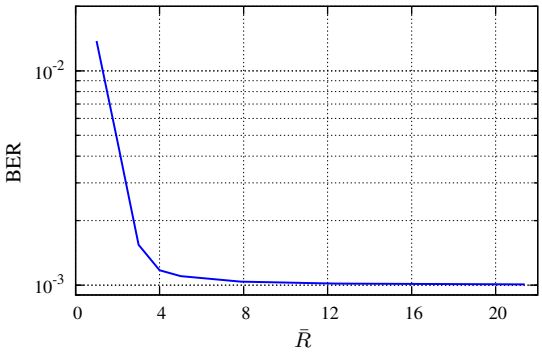

Fig. 5. BER versus mean number of S-LSQR recursions, for $M/N = 34.7\%$ and an SNR of 12 dB.

T and S-LSQR-T, respectively. For M/N increasing up to 39%, the SNR loss of LSQR rises to about 1.2 dB, as opposed to less than 0.2 dB for S-LSQR. This again shows that the DFE using the S-LSQR algorithm does not suffer from error propagation.

BER versus number of recursions. Finally, Fig. 5 shows the BER versus the mean number of S-LSQR recursions, for $M/N = 34.7\%$, SNR $= 12$ dB, $T_1 = 1.4$, and different values of ε. For each ε, we performed 5000 simulation runs and calculated the corresponding BER and the mean number of S-LSQR recursions (denoted $\bar{R}$). It is seen that the BER drops with growing $\bar{R}$ but levels off after about $\bar{R} = 4$. Hence, the performance gain of the S-LSQR algorithm relative to the LSQR algorithm can be leveraged already with a small number of recursions and, thus, a complexity that is not dramatically larger than that of the LSQR algorithm.

5. CONCLUSION

We proposed an ICI/ISI equalizer that is especially suited for multicarrier transmissions over rapidly time-varying and strongly delay-spread channels. A decision-feedback structure cancels postcursor ISI, while ICI is equalized by a sequential version of the LSQR algorithm. Low complexity is obtained by exploiting the approximate bandedness of the frequency-domain channel matrix. The sequential LSQR algorithm combines the LSQR algorithm with a generalized SPIC scheme that uses reliability-based sorting of sets of symbols (subcarriers). Simulation results demonstrated the excellent performance of the proposed ICI/ISI equalizer already for a small number of detecting-and-cancelling recursions.

6. REFERENCES

[1] S. Tomasin, A. Gorokhov, H. Yang, and J. P. Linnartz, "Iterative interference cancellation and channel estimation for mobile OFDM," *IEEE Trans. Wireless Comm.*, vol. 4, pp. 238–245, Jan. 2005.

[2] W. Kozek and A. F. Molisch, "Nonorthogonal pulseshapes for multicarrier communications in doubly dispersive channels," *IEEE J. Sel. Areas Comm.*, vol. 16, pp. 1579–1589, Oct. 1998.

[3] G. Matz, D. Schafhuber, K. Gröchenig, M. Hartmann, and F. Hlawatsch, "Analysis, optimization, and implementation of low-interference wireless multicarrier systems," *IEEE Trans. Wireless Comm.*, vol. 6, pp. 1921–1931, May 2007.

[4] G. Tauböck, M. Hampejs, G. Matz, F. Hlawatsch, and K. Gröchenig, "LSQR-based ICI equalization for multicarrier communications in strongly dispersive and highly mobile environments," in *Proc. IEEE SPAWC 2007*, (Helsinki, Finland), June 2007.

[5] R. Haas and J. C. Belfiore, "A time-frequency well-localized pulse for multiple carrier transmission," *Wireless Personal Comm.*, vol. 5, pp. 1–18, 1997.

[6] T. Strohmer and S. Beaver, "Optimal OFDM design for time-frequency dispersive channels," *IEEE Trans. Comm.*, vol. 51, pp. 1111–1122, July 2003.

[7] P. Schniter, "On the design of non-(bi)orthogonal pulse-shaped FDM for doubly-dispersive channels," in *Proc. IEEE ICASSP-2004*, vol. 3, (Montreal, Canada), pp. 817–820, 2004.

[8] S. Das and P. Schniter, "Max-SINR ISI/ICI-shaping multicarrier communication over the doubly dispersive channel," *IEEE Trans. Signal Processing*, vol. 55, no. 12, pp. 5782–5795, 2007.

[9] Y.-S. Choi, P. J. Voltz, and F. A. Cassara, "On channel estimation and detection for multicarrier signals in fast and selective Rayleigh fading channels," *IEEE Trans. Comm.*, vol. 49, pp. 1375–1387, Aug. 2001.

[10] X. Cai and G. B. Giannakis, "Bounding performance and suppressing intercarrier interference in wireless mobile OFDM," *IEEE Trans. Comm.*, vol. 51, pp. 2047–2056, Dec. 2003.

[11] L. Rugini, P. Banelli, and G. Leus, "Simple equalization of time-varying channels for OFDM," *IEEE Comm. Letters*, vol. 9, pp. 619–621, July 2005.

[12] T. Hrycak and G. Matz, "Low-complexity time-domain ICI equalization for OFDM communications over rapidly varying channels," in *Proc. Asilomar Conf. Signals, Systems, Computers*, (Pacific Grove, CA), pp. 1767–1771, Oct.-Nov. 2006.

[13] C. C. Paige and M. A. Saunders, "LSQR: An algorithm for sparse linear equations and sparse least squares," *ACM Trans. Math. Software*, vol. 8, pp. 43–71, March 1982.

[14] Y. Sun, "Bandwidth-efficient wireless OFDM," *IEEE J. Sel. Areas Comm.*, vol. 19, no. 11, pp. 2267–2278, 2001.

[15] L. Rugini, P. Banelli, R. C. Cannizzaro, and G. Leus, "Channel estimation and windowed DFE for OFDM with Doppler spread," in *Proc. IEEE ICASSP-2006*, vol. IV, pp. 137–140, May 2006.

[16] R. Fantacci, "Proposal of an interference cancellation receiver with low complexity for DS/CDMA mobile communication systems," *IEEE Trans. Veh. Technol.*, vol. 48, no. 4, pp. 1039–1046, 1999.

[17] J. Cai, J. Mark, and X. Shen, "ICI cancellation in OFDM wireless communication systems," in *Proc. IEEE GLOBECOM-2002*, vol. 1, pp. 656–660, 2002.

[18] K. Liu, T. Kadous, and A. M. Sayeed, "Orthogonal time-frequency signaling over doubly dispersive channels," *IEEE Trans. Inf. Theory*, vol. 50, no. 11, pp. 2583–2603, 2004.

[19] S. J. Hwang and P. Schniter, "Efficient sequence detection of multicarrier transmissions over doubly dispersive channels," *EURASIP J. Appl. Signal Processing*, vol. 2006, pp. 1–17, 2006.

[20] G. H. Golub and C. F. Van Loan, *Matrix Computations*. Baltimore: Johns Hopkins University Press, 3rd ed., 1996.

[21] P. C. Hansen, *Rank-Deficient and Discrete Ill-Posed Problems: Numerical Aspects of Linear Inversion*. Philadelphia, PA: SIAM, 1998.

[22] P. Schniter and S. D'Silva, "Low-complexity detection of OFDM in doubly-dispersive channels," in *Proc. Asilomar Conf. Signals, Systems, Computers*, vol. 2, pp. 1799–1803, 2002.

[23] P. Schniter, "Low-complexity equalization of OFDM in doubly-selective channels," *IEEE Trans. Signal Processing*, vol. 52, pp. 1002–1011, April 2004.

[24] M. Chiani, "Introducing erasures in decision-feedback equalization to reduce error propagation," *IEEE Trans. Comm.*, vol. 45, no. 7, pp. 757–760, 1997.

[25] P. A. Bello, "Characterization of randomly time-variant linear channels," *IEEE Trans. Comm. Syst.*, vol. 11, pp. 360–393, 1963.

[26] P. Schniter, "A new approach to multicarrier pulse design for doubly-dispersive channels," in *Proc. Annual Allerton Conference on Communication Control and Computing*, vol. 2, pp. 1012–1021, 2003.

[27] D. Schafhuber, G. Matz, and F. Hlawatsch, "Simulation of wideband mobile radio channels using subsampled ARMA models and multistage interpolation," in *Proc. 11th IEEE Workshop on Statistical Signal Processing*, (Singapore), pp. 571–574, Aug. 2001.